

Studies on Melt Spinning. III. Flow Instabilities in Melt Spinning: Melt Fracture and Draw Resonance

CHANG DAE HAN and RONALD R. LAMONTE,
*Department of Chemical Engineering, Polytechnic Institute of Brooklyn,
Brooklyn, New York 11201* and YATISH T. SHAH, *Department of Chemical
Engineering, University of Pittsburgh, Pittsburgh, Pennsylvania 15213*

Synopsis

An experimental study has been carried out to investigate threadline instabilities in melt spinning. Two types of melt threadline instabilities, draw resonance and melt fracture, were observed under both isothermal and nonisothermal spinning conditions. Polymers investigated were polypropylene and polystyrene. Draw resonance was observed as an increase of the take-up speed above a critical value. It was also observed that an increase in take-up speed reduces the severity of melt fracture, whereas once draw resonance occurs the amplitude and frequency of the pulsing thread diameter increases with the take-up speed. The phenomenon of draw resonance was investigated by taking motion pictures of the pulsing molten threadline spun vertically downward. Furthermore, a stability analysis was carried out to explain the experimentally observed draw resonance.

INTRODUCTION

It has been a concern of the fiber industry to carefully avoid producing a nonuniform thread diameter which is detrimental to textile processing. Two types of phenomenon resulting in nonuniform thread diameter have been observed in melt spinning. One is typically cyclic in nature, the so-called "draw resonance." The other is distortion of the extrudate surface, with a severity ranging from simple roughness to helical indentations. This is called "melt fracture."

During the past decade, much effort has been spent on investigating the cause (or causes) of these two phenomena, which we shall refer to as melt flow instabilities. According to the literature, the occurrence of each of these two flow instabilities arises from different processing conditions. That is, melt fracture starts to occur at some critical value of throughput rate even in the *absence* of thread stretching, whereas draw resonance starts to occur only in the *presence* of thread stretching. It should be noted therefore that both melt fracture and draw resonance limit productivity in melt spinning.

Freeman and Coplan¹ have studied unstable flow in fiber spinning. They have concluded, on the basis of their spinning experiments, that melt inhomogeneity may be responsible for periodic bulging along the spinline

(draw resonance). Draw resonance was also studied by Bergonzoni and Di-Cresce² who reported that there is a critical speed ratio (take-up speed/die exit speed) at which the thread cross section becomes periodic. Using a ribbon die, they correlated the width ratio (largest diameter/smallest diameter) with the speed ratio for different polymers and found that it increased with speed ratio until thread breakdown occurs. These authors reported further that the thread always broke at the water-air interface, and then concluded that frictional heating (due to molecules sliding past one another) is responsible for draw resonance. Therefore, it has been understood in general that draw resonance is closely related to the spinning conditions in the presence of stretching.

Some attempts at explaining the occurrence of draw resonance theoretically have been made by Pearson and his co-workers. Pearson and Matovich³ carried out a linearized stability analysis of Newtonian fluids subject to isothermal spinning conditions. More recently, Shah and Pearson^{4,5} extended the earlier approach of Pearson and Matovich by considering a Newtonian fluid subject to nonisothermal spinning and a power law fluid under isothermal spinning.

On the other hand, the occurrence of melt fracture has largely been investigated in connection with die design itself, namely, the entrance geometry of a die and the length-to-diameter ratio of a circular capillary.⁶⁻¹¹ Of particular interest has been the choice of the proper die entry angle from a processing point of view, so that dead space outside the converging melt streamlines in the reservoir might be eliminated. This die geometry has been proved to control the critical shear rate.

In the present paper, which is the third of this series, we shall discuss our recent experimental observations made on flow instability phenomena in melt spinning (i.e., melt fracture and draw resonance) and present a theoretical analysis for explaining the experimentally observed phenomenon of draw resonance.

EXPERIMENTAL OBSERVATIONS ON FLOW INSTABILITIES IN MELT SPINNING

The spinning apparatus used was the same as that described in an earlier paper by Han and Lamonte.¹² In the present study, however, a movie camera (Bolex Super 8) was also used in order to take motion pictures of the pulsing threadline when the phenomenon of draw resonance was observed.

The Phenomenon of Melt Fracture in Spinning

It has been known for a long time to the polymer processing industry that polymers, when melted and extruded through a die, can give rise to a distorted extrudate at and above a certain shear rate in the die. It has also been known that the severity of extrudate distortion varies from roughness of surface to helical indentations, depending on the materials being extruded, the geometry of dies, and the extrusion conditions. This phenom-

enon has been referred to as "melt fracture." During the past decade, a number of researchers⁶⁻¹¹ have tried to obtain a better understanding of the cause (or causes) of melt fracture. Up to the present time, unfortunately, no complete agreement has been seen among researchers on any particular mechanism proposed for explaining the phenomenon occurring.

It should be noted further that many of the studies on melt fracture in the past were concerned with the phenomenon occurring in plastics extrusion, but very little in fiber spinning. The main difference between the two lies in that, in fiber spinning, the molten extrudate is continuously pulled away from the die by means of a take-up device, whereas in plastics extrusion, the molten extrudate flows freely into quiescent ambient air and becomes solidified. There, then, an interesting question yet unanswered arises as to whether the action of pullaway would enhance the severity of extrudate distortion or not. One purpose of the experiments reported here was just to answer this curious question, in view of the importance of the problem in commercial melt spinning.

TABLE I
Summary of Spinning Conditions for Melt Fracture Experiment^a

| Code of pictures | Take-up velocity, m/min | Apparent stretch ratio ^b | True stretch ratio ^c |
|------------------|-------------------------|-------------------------------------|---------------------------------|
| (a) | 0.0 (gravity) | 0.00 | 0.00 |
| (b) | 3.3 | 0.31 | 2.79 |
| (c) | 9.5 | 0.90 | 8.10 |
| (d) | 25.3 | 2.40 | 21.60 |

^a Material = polystyrene (Styron 686); throughput rate = 8.3 gm/min; average velocity in the spinnerette hole ($V_0 = 10.55$ m/min; diameter of spinnerette hole = 1 mm; melt temperature = 180°C; apparent shear rate in the spinnerette hole = 1410 sec⁻¹).

^b Based on the velocity in the spinnerette (V_L/V_0).

^c Based on the approximately calculated initial velocity at the position where the maximum die swell occurred (V_L/V_f).

General-purpose polystyrene (Dow Chemical Co., Styron 686) was used in studying the effect of stretch rate on the severity of melt fracture. From a practical point of view, there are two spinning variables by means of which one can control the occurrence of melt fracture. For a fixed geometry of spinnerette hole, these are shear rate and melt temperature. More specifically stated, an increase in shear rate at a fixed melt temperature will eventually bring the inception of melt fracture at some critical value of shear rate, and a decrease in melt temperature will lower the critical shear rate. In our spinning experiment, we had to find a temperature by a trial-and-error method, which would then permit us to observe smooth threadline at low shear rates, but distorted threadline at high shear rates over the range of pumping rates which were available to us. One such temperature we found was 180°C, and this was the temperature at which the results shown below were obtained. Table I gives a summary of the spinning conditions used in the melt fracture experiment.

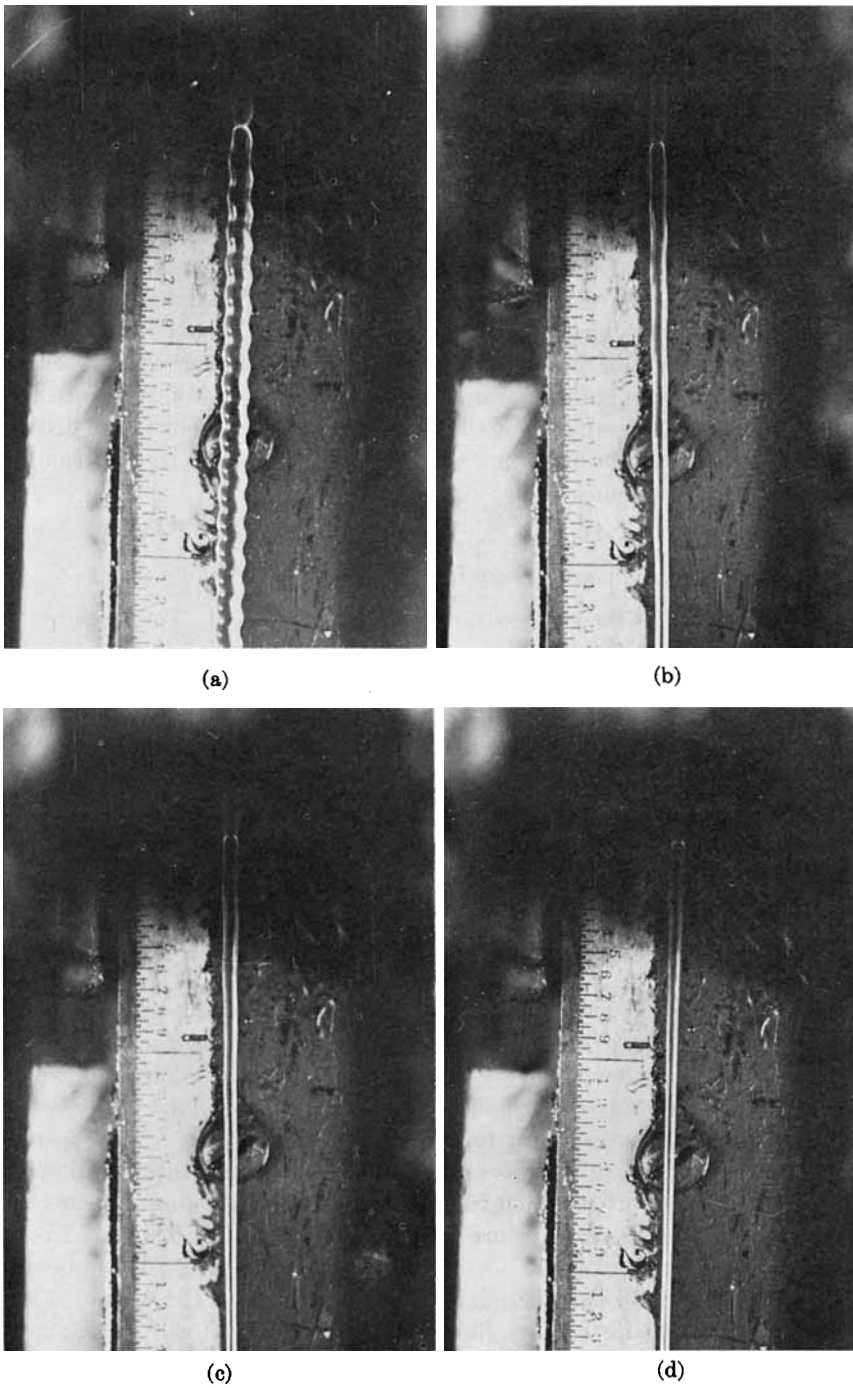


Fig. 1. Pictures of polystyrene threadlines being spun under melt fracture condition: (a) under gravity flow (i.e., no stretching); (b) at $V_L/V_0 = 0.31$; (c) at $V_L/V_0 = 0.90$; (d) at $V_L/V_0 = 2.40$.

Figure 1 shows representative pictures taken of a threadline spun vertically downward into ambient air, at four different stretching conditions: Figure 1a, under gravity alone (i.e., no stretching); Figure 1b, at an apparent stretch ratio of 0.316; Figure 1c, at an apparent stretch ratio of 0.901; and Figure 1d, at an apparent stretch ratio of 2.4. A few things are worth mentioning about these pictures. First, since the spinnerette was located at about 7 feet above the floor, even under gravity alone the severity of melt fracture of a molten threadline a few inches below the spinnerette face was different, depending on the length of the threadline hanging between the spinnerette face and the floor. Figure 1a is a picture taken of a threadline at the instant when about a 4-in. length hung below the spinnerette. Now, as may be seen from the rest of the pictures in Figure 1, the severity of melt fracture decreases very rapidly as the stretch rate increases. Thus, in Figure 1d, a mild distortion is seen in the molten threadline within the distance of 1 in. below the spinnerette. This mild distortion almost completely disappeared as the threadline traveled downward several feet more under stretching. Then, from a practical point of view, the obvious question is, what does the final threadline look like after it solidifies and is wound up on the take-up roller? Figure 2 shows pictures taken of the solidified threadlines. It may be said, from Figure 2e, that at an apparent stretch ratio of 2.4 the final thread is virtually free of distortion. This is a very important fact to the fiber manufacturer.

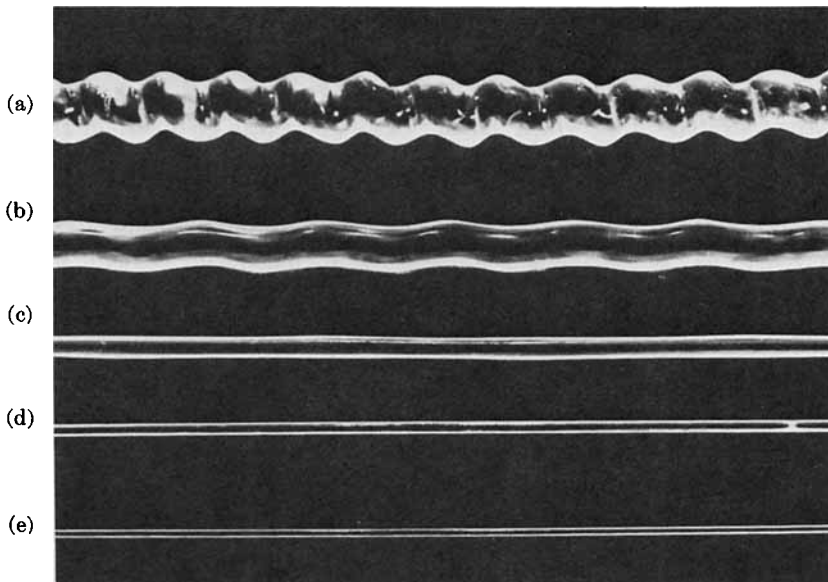


Fig. 2. Pictures of polystyrene fibers: (a) collected at 4 in. from the spinnerette face without stretching; (b) collected at about 6 feet from the spinnerette face without stretching; (c) spun at $V_L/V_0 = 0.31$; (d) spun at $V_L/V_0 = 0.90$; (e) spun at $V_L/V_0 = 2.40$.

However, it should be remembered that, once melt fracture occurs, it limits the maximum allowable stretch ratio. The reason is that at excessive stretch rates the molten threadline might break near the spinnerette. Yet, what Figures 1 and 2 tell us is that melt fracture depends purely on the flow conditions inside the spinnerette and that the severity of melt fracture can virtually be eliminated in the final threadline by judiciously choosing its stretch rate and possibly its cooling rate when molten.

Finally, it should be noted that, in Figures 1 and 2, the apparent stretch ratios were stated in order to give some idea of the velocity of the solidified threadline at the take-up device relative to its initial velocity. The initial velocity should be taken as the velocity of a molten threadline somewhere outside the spinnerette. Such a value may be calculated from the measurement of the diameter of a completely relaxed thread with no gravity effect. Using the mass balance

$$V_f = V_1(D_f/D_1)^2 \quad (1)$$

where V_1 is the average velocity in the spinnerette hole, D_f is the relaxed thread diameter, D_1 is the spinnerette hole diameter, and V_f is the free jet velocity at the position where D_f is determined. However, there is a practical difficulty in accurately determining a value of D_f which is free of gravity effect. What we could do at best was to take photographs of a very short extrudate length, cutting the molten threadline so that the gravity effect might be minimized. Having done this, we were able to obtain our best estimate of V_f/V_1 as about 9 from the measurement of die swell ratio (D_f/D_1), which was about 3.

Based on this estimate, we have given in Table I the true stretch ratios. We have done this in order not to mislead readers when they see the apparent stretch ratios, which in some cases happen to be less than 1.0.

The Phenomenon of Draw Resonance in Melt Spinning

The phenomenon of pulsation of thread diameter in extrusion has been referred to as "draw resonance." Earlier, Freeman and Coplan¹ reported their observations made on this phenomenon during melt spinning, and Bergonzoni and DiCresce² also observed basically the same phenomenon in film extrusion, where a ribbon die was used with a quenching water bath. What makes the phenomenon of draw resonance most interesting, and also distinct from the phenomenon of melt fracture, is that it starts to occur *only* when the stretch ratio reaches a certain critical value at a fixed throughput rate. The severity of thread pulsation then increases as the stretch ratio is further increased beyond the critical value, ultimately leading to a breakdown of threadline.

Strange as it may seem, polypropylene is one of the very few polymers which are reported in the literature to have exhibited draw resonance. On the other hand, melt fracture has been observed with almost all the polymers commercially available. In the present study, polypropylene (Enjay Chemical Co., Resin E115) was used. In fact, our efforts to obtain draw

resonance with high-density polyethylene, low-density polyethylene, and polystyrene were quite unsuccessful. This is not to say that polypropylene is the only polymer which exhibits the phenomenon.

Although it was not clearly stated in the literature,^{1,2} we have found that draw resonance occurs at and above a certain throughput rate. At low throughput rates, increasing the stretch rate caused thread breakage before any thread pulsation was seen. However, a gradual increase in throughput rate permitted us to observe pulsing threadline at some reasonable stretch ratios, and then the severity of thread pulsation increased as the stretch rate was further increased. Ultimately, this led to thread breakdown. Interestingly enough, we have also noticed that, under the identical throughput rate and stretch ratio, spinning into ambient air (i.e., nonisothermal spinning) gives rise to much more severe draw resonance than spinning into an isothermal chamber. More will be said later about the effect of air temperature on the severity of draw resonance.

A series of motion pictures of pulsing threadline was taken under various spinning conditions of throughput rate, stretch rate, and air temperature. A summary of the spinning conditions is given in Table II. In order to quantitatively examine the variations of pulsing fiber diameter, the thread diameter was read off from the projected images of the motion pictures. This was done by stopping the projector at every fourth frame, which corresponds to $\frac{2}{9}$ of a second in real time. Tables III through V give the diameter readings at three stretch ratios: 23.2, 39.3, and 83.5.

TABLE II
Summary of Spinning Conditions for Draw Resonance Experiment

| |
|---|
| Material = polypropylene (Enjay Resin E115) |
| Throughput rate = 2.94 g/min |
| Average velocity in the spinnerette hole (V_0) = 5.21 m/min |
| Diameter of spinnerette hole = 1 mm |
| Melt temperature = 180°C |
| Air temperature = room temperature (25°C) |

Figure 3 shows plots versus time of the ratio of diameter-to-average diameter [$d(t)/\bar{d}$] for the pulsing thread at various stretching conditions at a distance of 0.2 in. from the spinnerette face. It is seen from these plots that the amplitude of a pulsing threadline increases with stretch ratio. In Table VI are given the average amplitude (deviation) and average frequency of a pulsing threadline as a function of apparent stretch ratio. At higher stretch ratios, a breakage of threadline was experienced during the experiment, and this can now be explained from Figure 3.

There are two important aspects of the problem which are worth elaborating. First, the thread breakage mechanism in the presence of draw resonance is believed to be quite different from that of a free liquid jet. The latter has been much discussed in the literature.^{13,14} Ziabicki¹³ proposed a so-called "capillary breakup" mechanism in defining a criterion of spinnabil-

TABLE III
Thread Diameters in the Presence of Draw
Resonance at an Apparent Stretch Ratio of 23.2

| Time, sec | Thread diameter, in. | | |
|-----------|----------------------|---------------|---------------|
| | $X^a = 0.2$ in. | $X = 0.4$ in. | $X = 0.6$ in. |
| 0.0000 | 0.0778 | 0.0831 | 0.0855 |
| 0.2222 | 0.0817 | 0.0802 | 0.0807 |
| 0.4444 | 0.0807 | 0.0817 | 0.0822 |
| 0.6666 | 0.0795 | 0.0818 | 0.0813 |
| 0.8888 | 0.0776 | 0.0813 | 0.0809 |
| 1.1111 | 0.0804 | 0.0818 | 0.0827 |
| 1.3333 | 0.0790 | 0.0800 | 0.0823 |
| 1.5555 | 0.0825 | 0.0830 | 0.0863 |
| 1.7777 | 0.0825 | 0.0839 | 0.0858 |
| 2.0000 | 0.0801 | 0.0830 | 0.0830 |
| 2.2222 | 0.0783 | 0.0839 | 0.0830 |
| 2.4444 | 0.0789 | 0.0808 | 0.0836 |
| 2.6666 | 0.0789 | 0.0822 | 0.0787 |
| 2.8888 | 0.0780 | 0.0785 | 0.0822 |
| 3.1111 | 0.0803 | 0.0799 | 0.0817 |
| 3.3333 | 0.0771 | 0.0789 | 0.0780 |
| 3.5555 | 0.0798 | 0.0807 | 0.0812 |
| 3.7777 | 0.0802 | 0.0807 | 0.0812 |
| 4.0000 | 0.0802 | 0.0798 | 0.0812 |
| 4.2222 | 0.0822 | 0.0841 | 0.0836 |
| 4.4444 | 0.0788 | 0.0812 | 0.0865 |
| 4.6666 | 0.0774 | 0.0798 | 0.0831 |
| 4.8888 | 0.0783 | 0.0774 | 0.0798 |
| 5.1111 | 0.0812 | 0.0817 | 0.0841 |
| 5.3333 | 0.0803 | 0.0842 | 0.0851 |
| 5.5555 | 0.0813 | 0.0794 | 0.0818 |
| 5.7777 | 0.0818 | 0.0827 | 0.0846 |
| 6.0000 | 0.0808 | 0.0803 | 0.0827 |
| 6.2222 | 0.0827 | 0.0832 | 0.0856 |
| 6.4444 | 0.0799 | 0.0818 | 0.0837 |
| 6.6666 | 0.0813 | 0.0837 | 0.0851 |
| 6.8888 | 0.0773 | 0.0796 | 0.0800 |
| 7.1111 | 0.0787 | 0.0805 | 0.0805 |
| 7.3333 | 0.0782 | 0.0824 | 0.0828 |
| 7.5555 | 0.0759 | 0.0773 | 0.0777 |
| 7.7777 | 0.0791 | 0.0800 | 0.0782 |

^a X is distance from spinnerette face.

ity. In the breakup of a free liquid jet into droplets, a wavy jet surface is formed upon exiting from the nozzle, where no action of stretching is imposed on the jet. Undoubtedly, the surface tension force plays an important role in the formation of a wavy jet surface. A recent study of Goldin et al.¹⁴ has treated this problem very elegantly. However, as stated above, the onset of draw resonance occurs only at a certain critical value of stretch ratio (see Fig. 3). Therefore, a theoretical study on the phenomenon should take into account the stretch ratio as an important boundary condi-

TABLE IV
Thread Diameters in the Presence of Draw Resonance
at an Apparent Stretch Ratio of 39.3

| Time, sec | Thread diameter, in. | | |
|-----------|----------------------|---------------|---------------|
| | $X^a = 0.2$ in. | $X = 0.4$ in. | $X = 0.6$ in. |
| 0.0000 | 0.0823 | 0.0819 | 0.0819 |
| 0.2222 | 0.0769 | 0.0796 | 0.0828 |
| 0.4444 | 0.0823 | 0.0819 | 0.0805 |
| 0.6666 | 0.0819 | 0.0737 | 0.0787 |
| 0.8888 | 0.0819 | 0.0773 | 0.0800 |
| 1.1111 | 0.0773 | 0.0719 | 0.0733 |
| 1.3333 | 0.0840 | 0.0784 | 0.0784 |
| 1.5555 | 0.0769 | 0.0802 | 0.0807 |
| 1.7777 | 0.0774 | 0.0802 | 0.0826 |
| 2.0000 | 0.0802 | 0.0807 | 0.0816 |
| 2.2222 | 0.0798 | 0.0798 | 0.0816 |
| 2.4444 | 0.0774 | 0.0798 | 0.0784 |
| 2.6666 | 0.0812 | 0.0826 | 0.0859 |
| 2.8888 | 0.0709 | 0.0731 | 0.0768 |
| 3.1111 | 0.0777 | 0.0750 | 0.0818 |
| 3.3333 | 0.0763 | 0.0768 | 0.0754 |
| 3.5555 | 0.0781 | 0.0795 | 0.0786 |
| 3.7777 | 0.0835 | 0.0816 | 0.0806 |
| 4.0000 | 0.0821 | 0.0801 | 0.0830 |
| 4.2222 | 0.0763 | 0.0801 | 0.0797 |
| 4.4444 | 0.0801 | 0.0821 | 0.0797 |
| 4.6666 | 0.0777 | 0.0801 | 0.0806 |
| 4.8888 | 0.0797 | 0.0811 | 0.0855 |
| 5.1111 | 0.0811 | 0.0830 | 0.0850 |
| 5.3333 | 0.0816 | 0.0835 | 0.0864 |
| 5.5555 | 0.0826 | 0.0879 | 0.0847 |
| 5.7777 | 0.0819 | 0.0868 | 0.0853 |
| 6.0000 | 0.0800 | 0.0829 | 0.0848 |
| 6.2222 | 0.0790 | 0.0814 | 0.0829 |
| 6.4444 | 0.0790 | 0.0819 | 0.0839 |
| 6.6666 | 0.0780 | 0.0809 | 0.0824 |
| 6.8888 | 0.0809 | 0.0824 | 0.0848 |
| 7.1111 | 0.0834 | 0.0848 | 0.0858 |
| 7.3333 | 0.0829 | 0.0843 | 0.0902 |
| 7.5555 | 0.0775 | 0.0814 | 0.0843 |
| 7.7777 | 0.0785 | 0.0804 | 0.0834 |
| 8.0000 | 0.0795 | 0.0804 | 0.0853 |

^a X is distance from spinnerette face.

tion. This problem will be treated below in an attempt to explain our experimental observations.

Second, it has been observed that the severity of the resonant behavior of the thread diameter was enhanced when melt was spun into ambient air (25°C), rather than into an isothermal chamber whose temperature was maintained the same as that of the melt itself (180°C). The temperature effect was more dramatically demonstrated when air was blown gently

TABLE V
Thread Diameters in the Presence of Draw Resonance
at an Apparent Stretch Ratio of 83.5

| Time, sec | Thread diameter, in. | | |
|-----------|----------------------|---------------|---------------|
| | $X^* = 0.2$ in. | $X = 0.4$ in. | $X = 0.6$ in. |
| 0.0000 | 0.0818 | 0.0813 | 0.0823 |
| 0.2222 | 0.0813 | 0.0857 | 0.0843 |
| 0.4444 | 0.0862 | 0.0848 | 0.0862 |
| 0.6666 | 0.0813 | 0.0813 | 0.0843 |
| 0.8888 | 0.0862 | 0.0843 | 0.0857 |
| 1.1111 | 0.0838 | 0.0828 | 0.0818 |
| 1.3333 | 0.0857 | 0.0848 | 0.0872 |
| 1.5555 | 0.0819 | 0.0834 | 0.0864 |
| 1.7777 | 0.0869 | 0.0844 | 0.0834 |
| 2.0000 | 0.0859 | 0.0854 | 0.0879 |
| 2.2222 | 0.0751 | 0.0779 | 0.0793 |
| 2.4444 | 0.0784 | 0.0779 | 0.0774 |
| 2.6666 | 0.0812 | 0.0847 | 0.0857 |
| 2.8888 | 0.0862 | 0.0852 | 0.0857 |
| 3.1111 | 0.0812 | 0.0857 | 0.0837 |
| 3.3333 | 0.0847 | 0.0832 | 0.0827 |
| 3.5555 | 0.0837 | 0.0832 | 0.0862 |
| 3.7777 | 0.0847 | 0.0847 | 0.0847 |
| 4.0000 | 0.0812 | 0.0807 | 0.0832 |
| 4.2222 | 0.0807 | 0.0832 | 0.0837 |
| 4.4444 | 0.0812 | 0.0812 | 0.0817 |
| 4.6666 | 0.0842 | 0.0847 | 0.0898 |
| 4.8888 | 0.0827 | 0.0837 | 0.0868 |
| 5.1111 | 0.0860 | 0.0865 | 0.0865 |
| 5.3333 | 0.0870 | 0.0844 | 0.0870 |
| 5.5555 | 0.0870 | 0.0844 | 0.0881 |
| 5.7777 | 0.0870 | 0.0865 | 0.0887 |
| 6.0000 | 0.0826 | 0.0821 | 0.0850 |
| 6.2222 | 0.0835 | 0.0830 | 0.0859 |
| 6.4444 | 0.0806 | 0.0811 | 0.0826 |
| 6.6666 | 0.0877 | 0.0806 | 0.0821 |
| 6.8888 | 0.0816 | 0.0792 | 0.0845 |
| 7.1111 | 0.0806 | 0.0811 | 0.0845 |
| 7.3333 | 0.0806 | 0.0821 | 0.0811 |
| 7.5555 | 0.0801 | 0.0821 | 0.0816 |
| 7.7777 | 0.0821 | 0.0811 | 0.0850 |
| 8.0000 | 0.0792 | 0.0801 | 0.0801 |

* X is distance from spinnerette face.

crosscurrently to a spinline which was already in a mildly resonant state. This air flow gradually increased the severity of thread pulsation and led to breakage. Therefore, our experiment has clearly demonstrated that the faster cooling of a molten threadline in the resonance state *destabilizes* the flow in elongational flow. In fact, earlier, Kase and Matsuo¹⁵ demonstrated similar behavior theoretically in their analysis of the unsteady-state behavior of molten threadlines. Based on our own observations, we can say

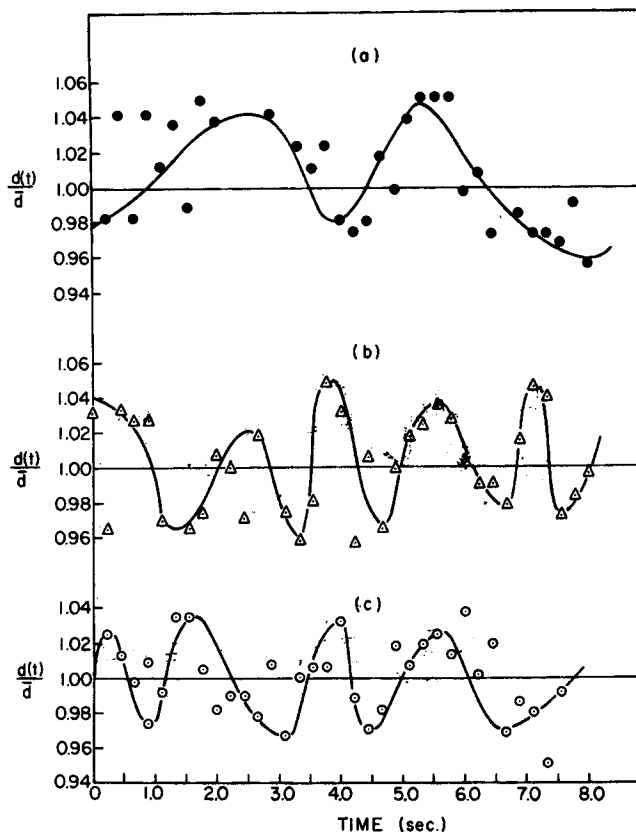


Fig. 3. Plots of normalized fiber diameter, $d(t)/\bar{d}$, vs. time for a pulsing polypropylene thread at various stretching conditions at a distance of 0.2 in. from the spinnerette face: (a) at $V_L/V_0 = 23.2$; (b) at $V_L/V_0 = 39.3$; (c) at $V_L/V_0 = 83.5$.

that the elasticity of a melt destabilizes the resonant type of melt flow. That is because cooling a molten threadline brings a increase in both viscosity and elasticity. However, it has long been a well-known fact that viscosity *enhances* flow stability by damping out the disturbances introduced into the fluid.¹⁶

The fact that the elasticity of a fluid tends to destabilize flow is not new. In the past, Thomas and Walters^{17,18} and Herbert¹⁹ have contended that

TABLE VI
Average Amplitude and Frequency of a Pulsing Threadline at
 $X = 0.2$ in. from Spinnerette Face

| Apparent stretch ratio | Average amplitude (deviation) | Average frequency, sec^{-1} |
|------------------------|-------------------------------|--------------------------------------|
| 23.2 | 0.030 | 0.54 |
| 39.3 | 0.036 | 0.56 |
| 83.5 | 0.053 | 0.285 |

fluid elasticity *destabilizes* the motion of viscoelastic fluids in couette flow between two coaxial cylinders. On the other hand, in a recent experiment on the breakup of liquid jets, Goldin et al.¹⁴ demonstrated that fluid elasticity *stabilizes* the motion of viscoelastic liquid jets. It appears then, that the role of fluid elasticity in either stabilizing or destabilizing a motion of viscoelastic liquids depends on the type of flow field, and therefore a generalization is probably not practically possible.

It seems clear, then, that a theoretical study is needed for the better understanding of the role of fluid elasticity in the resonant behavior of a viscoelastic polymer melt. Pearson and Matovich³ have speculated that fluid elasticity would stabilize the resonant behavior of molten threadlines, a view quite opposite to the experimental observations reported in this paper. The conclusion drawn by Pearson and Matovich³ was based on an analysis using the second-order fluid due to Coleman and Noll.²⁰ In view of the inherent defects of the second-order fluid model in describing the elongational flow of polymer melts, a future study should perhaps be directed to a choice of more realistic models.

STABILITY ANALYSIS OF THE PHENOMENON OF DRAW RESONANCE

We shall present below, with some simplifying assumptions, a stability analysis of the phenomenon of draw resonance occurring in isothermal melt spinning. We shall consider isothermal spinning in order to avoid the mathematical complexities which may arise from considering both the equation of motion and the energy balance equation. However, considering the experimental evidence on the occurrence of draw resonance in isothermal spinning as discussed above, it should still yield valid explanation of the phenomenon.

The basic approach is essentially the same as that of Pearson and Matovich³ and Shah and Pearson.^{4,5} It makes use of the classical stability analysis dealing with linearized system equations. More specifically stated, we shall attempt to construct a region of stability in terms of stretch ratio and rheological properties of the fluid under consideration, by assuming a disturbance of the form $e^{i\omega t}$ introduced to the system. In other words, we look for the conditions under which the thread diameter grows exponentially with time in response to a disturbance of the form $e^{i\omega t}$.

The following assumptions are made: (1) the axial velocity distribution is predominant over the radial velocity distribution in a thread being stretched; (2) the elongation rate is small ($da/dx < 1$); and (3) a molten threadline being stretched travels through an isothermal chamber. The governing equation of motion and the equation of continuity may be written as follows^{3,5}:

$$\rho \left(\frac{\partial v}{\partial t} + v \frac{\partial v}{\partial x} \right) = \rho g + \frac{6\eta_E}{a} \frac{\partial a}{\partial x} \frac{\partial v}{\partial x} + 3\eta_E \frac{\partial^2 v}{\partial x^2} + 3 \frac{\partial \eta_E}{\partial x} \frac{\partial v}{\partial x} + \frac{\sigma}{a^2} \frac{\partial a}{\partial x} \quad (2)$$

and

$$\frac{\partial a}{\partial t} + v \frac{\partial a}{\partial x} + \frac{a}{2} \frac{\partial v}{\partial x} = 0, \quad (3)$$

respectively. In eqs. (2) and (3), ρ denotes the fluid density, g the acceleration of gravity, $v(x,t)$ the axial velocity of the threadline, $a(x,t)$ the radius of the thread, σ the surface tension of the fluid, and η_E the elongational viscosity, which is defined by

$$\eta_E = \frac{T_{xx}}{dv/dx} \quad (4)$$

where T_{xx} is the axial tensile stress and dv/dx is the elongation rate. It should be noted that η_E depends on x , also.

Now, in order to solve eqs. (2) and (3) for $v(x,t)$ and $a(x,t)$, one has first to specify η_E in terms of dv/dx . As discussed extensively in a previous paper,²¹ it appears to be a formidable task to correctly derive such an expression. Therefore, for our purposes, we shall rather choose an experimentally obtained expression, which for the spinning of polypropylene melts gives²¹

$$\eta_E = \eta_p \left(\frac{\partial v}{\partial x} \right)^{q-1} \quad (5)$$

where η_p and q are material constants. Referring to our earlier paper,²¹ there are other forms of power law model, more general than eq. (5). However, here we are concerned with polypropylene because it was the only polymer among several polymers tested which exhibited draw resonance. It should be noted also that very recently Shah and Pearson⁵ have carried out a stability analysis using the power law model, eq. (5), in eqs. (2) and (3). However, for completeness, we shall present below some essential steps which lead to the final working equations for stability analysis.

Introducing the following dimensionless variables

$$\begin{aligned} \xi &= x/L \\ \psi &= \bar{v}(x)/\bar{v}_0 \\ N_{Re} &= \rho L^q \bar{v}_0^{2-q} / 3\eta_p \\ N_{We} &= 2\rho \bar{a}_0 \bar{v}_0^2 / \sigma \\ \tau &= \bar{v}_0 t / L \\ N_{Fr} &= \bar{v}_0^2 / gL \end{aligned} \quad (6)$$

and the perturbation variables α and β , defined as

$$a(x,t) = \bar{a}(x)[1 + \alpha(x,t)] \quad (7)$$

$$v(x,t) = \bar{v}(x)[1 + \beta(x,t)] \quad (8)$$

eqs. (2) and (3) with the aid of eq. (5) will be rewritten as follows:

$$\begin{aligned}
 N_{Re} \left\{ \psi \frac{\partial \beta}{\partial \tau} + \psi^2 \frac{\partial \beta}{\partial \xi} \right\} &= q \psi \left(\frac{d\psi}{d\xi} \right)^{q-1} \frac{\partial^2 \beta}{\partial \xi^2} \\
 &+ \left[q \left(\frac{d\psi}{d\xi} \right)^q + q(q-1) \psi \left(\frac{d\psi}{d\xi} \right)^{q-2} \frac{d^2 \psi}{d\xi^2} \right] \frac{\partial \beta}{\partial \xi} + 2 \left(\frac{d\psi}{d\xi} \right)^q \frac{\partial \alpha}{\partial \xi} \\
 &+ \beta q \left[q \left(\frac{d\psi}{d\xi} \right)^{q-1} \frac{d^2 \psi}{d\xi^2} - \frac{1}{\psi} \left(\frac{d\psi}{d\xi} \right)^{q+1} - \frac{2N_{Re} \psi}{q} \left(\frac{d\psi}{d\xi} \right) \right] \\
 &+ \frac{N_{Re}}{N_{We}} \frac{1}{\psi^{1/2}} \frac{d\psi}{d\xi} \alpha + \frac{2N_{Re}}{N_{We}} \psi^{1/2} \frac{\partial \alpha}{\partial \xi} \quad (9)
 \end{aligned}$$

and

$$\frac{\partial \alpha}{\partial \tau} + \psi \frac{\partial \alpha}{\partial \xi} + \frac{\psi}{2} \frac{\partial \beta}{\partial \xi} = 0, \quad (10)$$

respectively. In the derivation of eqs. (9) and (10), it is assumed that terms higher than the first order in α , β , $\partial\alpha/\partial\tau$, $\partial\alpha/\partial\xi$, $\partial\beta/\partial\tau$, and $\partial\beta/\partial\xi$ are negligibly small compared to those of the first order. In eqs. (6)–(8), L denotes the length of spinline; \bar{v}_0 , the average velocity at $x = 0$ at steady state; $\bar{v}(x)$, the axial velocity profile at steady state; \bar{a}_0 , the radius of the thread at $x = 0$ at steady state; and $\bar{a}(x)$, the axial profile of the thread radius at steady state.

Two things are worth noting in eqs. (9) and (10). First, they are linear partial differential equations with variable coefficients. Those coefficients are to be determined from solving eqs. (2) and (3) by setting $\partial v/\partial t = 0$ and $\partial\alpha/\partial t = 0$. That is, one should solve for $\psi(\xi)$ from

$$\begin{aligned}
 q \psi \left(\frac{d\psi}{d\xi} \right)^{q-1} \frac{d^2 \psi}{d\xi^2} - \left(\frac{d\psi}{d\xi} \right)^{q+1} &= N_{Re} \psi^2 \frac{d\psi}{d\xi} \\
 - (N_{Re}/N_{Fr}) \psi + (N_{Re}/N_{We}) \psi^{1/2} \frac{d\psi}{d\xi} &\quad (11)
 \end{aligned}$$

which is obtained by first setting $\partial v/\partial t = \partial\alpha/\partial t = 0$ in eqs. (2) and (3) and then rewriting the resulting equations, by use of the proper variables defined in eq. (6) and also by use of eq. (5). Unfortunately, eq. (11) is a nonlinear differential equation whose solution would require some sort of numerical integration technique. In any case, it must first be solved for $\psi(\xi)$ in order to solve eqs. (9) and (10) for $\alpha(\xi, \tau)$ and $\beta(\xi, \tau)$, using proper boundary conditions.

Second, in view of the complicated expressions of eqs. (9) and (11), it would be worth examining the magnitude of each of their terms to see if there is any that might be small enough to be neglected. Referring to the spinning conditions (see Table II) under which draw resonance was actually observed in the spinning of polypropylene, we have the following estimates:

$$N_{Re} \simeq 9.75 \times 10^{-5}$$

$$N_{Fr} \simeq 3.99 \times 10^{-3}$$

$$N_{We} > 10$$

for which we have used the following values of η_p and q :

$$\eta_p = 1.62 \times 10^5 \text{ poise/sec}^{-0.883}$$

$$q = 0.117$$

as estimated in our earlier paper.²¹ Now, then, the magnitude analysis shows that eqs. (9) and (11) may be reduced to

$$q\psi \left(\frac{d\psi}{d\xi}\right)^{q-1} \frac{\partial^2 \beta}{d\xi^2} + \left[q \left(\frac{d\psi}{d\xi}\right)^q + q(q-1)\psi \left(\frac{d\psi}{d\xi}\right)^{q-2} \frac{d^2\psi}{d\xi^2} \right] \frac{\partial \beta}{d\xi} + 2 \left(\frac{d\psi}{d\xi}\right)^q \frac{\partial \alpha}{d\xi} = 0 \quad (12)$$

and

$$q\psi \left(\frac{d\psi}{d\xi}\right)^{q-1} \frac{d^2\psi}{d\xi^2} - \left(\frac{d\psi}{d\xi}\right)^{q+1} = 0, \quad (13)$$

respectively, when the terms containing N_{Re} , N_{Re}/N_{Fr} , and N_{Re}/N_{We} are neglected.

Boundary conditions have to be established for eq. (13) and initial and boundary conditions for eqs. (10) and (12). Boundary conditions for eq. (13) are readily given by

$$(i) \quad \text{at } \xi = 0, \psi(0) = 1 \quad (14)$$

$$(ii) \quad \text{at } \xi = 1, \psi(1) = \bar{v}_L/\bar{v}_0 \quad (15)$$

But as regards boundary conditions for eqs. (10) and (12), Pearson and Matovich³ have considered various possible ones in obtaining solutions of eqs. (10) and (12) for Newtonian fluids, i.e. $q = 1$. Although it is not impossible from a mathematical point of view to have more than one set of boundary and initial conditions which can give rise to draw resonance, it may not be possible from a practical point of view for us to observe draw resonance under more than one set. Of course, we do not know which of the different sets gives rise precisely to draw resonance in any practical situation. Therefore it appears that a choice must rely to a great extent on experience with actual experiments.

Based on our experience, we propose the following initial and boundary conditions:

$$(i) \quad \text{at } t = 0, \alpha(\xi, 0) = 0; \beta(\xi, 0) = 0 \quad (16)$$

$$(ii) \quad \text{at } \xi = 0, \alpha(0, \tau) = 0; \beta(0, \tau) = 0 \quad (17)$$

$$(iii) \quad \text{at } \xi = 1, \beta(1, \tau) = \sin \omega \tau \quad (18)$$

Boundary condition (18) suggests that a disturbance of the form $e^{i\omega\tau}$ is introduced at the take-up velocity in the thread at $\xi = 1$, which may then propagate upward through the already solidified threadline into the molten threadline near the spinnerette face. It should be noted that boundary conditions (17) and (18) are different from the boundary conditions used by Shah and Pearson.⁵

In the present study, eq. (13) with boundary conditions (14) and (15), and eqs. (10) and (12) with boundary and initial conditions (16)–(18) were solved numerically by following the same numerical technique as described in earlier work by Shah and Pearson.^{4,5} The technique consists of first transforming the differential equations into finite difference equations, then rearranging a set of large matrices in tridiagonal form, and finally performing the numerical computation. The details of the numerical computation are outlined in reference 5.

For $q = 0.117$, the lowest (or critical) value of the stretch ratio (\bar{v}_L/\bar{v}_0) at which a perturbation in radius at any nonzero axial distance would grow exponentially with time was determined on the computer by a trial-and-error procedure. The finite difference technique was found to be numerically stable for $\Delta\tau$ as high as 0.1. However, the numerical results for $\alpha(x,\tau)$ and $\beta(x,\tau)$ were obtained with maximum $\Delta\tau = 0.0005$ to ascertain the accuracy of results at all values of ω .^{4,5} The value of the critical stretch ratio obtained in this manner was found to be approximately 3.2.

Since no accurate experimental value of the critical stretch ratio is available at present, it is not possible to evaluate the validity of the above theoretical prediction. The value 3.2 for the critical stretch ratio is, however, close to the experimentally observed values of stretch ratio for which severe draw resonances were observed.

The theoretical calculations described above contain two assumptions which may have some effects on the accuracy of the critical stretch ratio. First, the stability analysis described above is a linearized stability analysis, i.e., the perturbation equations for α and β were derived neglecting the second- and higher-order terms in the perturbation variables. These terms may actually not be negligible. Secondly, the fluid rheological equation, eq. (5), used to describe the elongational flow of polypropylene does not contain a term for fluid elasticity. The fluid elasticity would, of course, have some effect on the stability or critical stretch ratio of the spinning process. Further theoretical studies are currently being pursued to evaluate the effect of fluid elasticity on the stability of the spinning process.

CONCLUSION

Two types of thread instability phenomena, melt fracture and draw resonance, were observed in melt spinning experiment.

It was observed that draw resonance (thread pulsation) occurs at and above a critical value of stretch ratio and that the amplitude and frequency of the pulsing diameter increases with the stretch ratio, ultimately leading to a breakdown of threadline.

On the other hand, it was observed that the severity of melt fracture (extrudate distortion) decreases very rapidly as the stretch ratio increases. This leads us to conclude that the severity of melt fracture can virtually be eliminated in the final threadline by judiciously choosing its stretch ratio.

Finally, a stability analysis was carried out to explain the experimentally observed draw resonance.

One of the authors (C.D.H.) gratefully acknowledges the support received from the National Science Foundation under Grant No. GK-23623.

References

1. H. I. Freeman and M. J. Coplan, *J. Appl. Polym. Sci.*, **8**, 2389 (1964).
2. A. Bergonzoni and A. J. DiCresce, *Polym. Eng. Sci.*, **6**, 45 (1966).
3. J. R. A. Pearson and M. A. Matovich, *Ind. Eng. Chem., Fundam.*, **8**, 605 (1969).
4. Y. T. Shah and J. R. A. Pearson, *Ind. Eng. Chem., Fundam.*, **11**, 145 (1972).
5. Y. T. Shah and J. R. A. Pearson, *Polym. Eng. Sci.*, **12**, 219 (1972).
6. J. P. Tordella, *J. Appl. Phys.*, **27**, 454 (1956).
7. J. P. Tordella, *Trans. Soc. Rheol.*, **1**, 203 (1957).
8. J. P. Tordella, *J. Appl. Polym. Sci.*, **7**, 215 (1963).
9. E. B. Bagley and H. P. Schreiber, *Trans. Soc. Rheol.*, **5**, 341 (1961).
10. G. A. Bialas and J. L. White, *Rubber Chem. Technol.*, **42**, 675 (1969).
11. C. D. Han and R. R. Lamonte, *Polym. Eng. Sci.*, **11**, 385 (1971).
12. C. D. Han and R. R. Lamonte, *Trans. Soc. Rheology*, **16**, 447 (1972).
13. A. Ziabicki, *Kolloid-Z.*, **198**, 60 (1964).
14. M. Goldin, J. Yerushalmi, R. Pfeffer, and R. Shinnar, *J. Fluid Mech.*, **38**, 689 (1969).
15. S. Kase and T. Matsuo, *J. Appl. Polym. Sci.*, **11**, 251 (1967).
16. S. Tomotika, *Proc. Roy. Soc.*, **A150**, 322 (1935).
17. R. H. Thomas and K. Walters, *Proc. Roy. Soc.*, **A274**, 371 (1963).
18. R. H. Thomas and K. Walters, *J. Fluid Mech.*, **18**, 33 (1964).
19. D. M. Herbert, *J. Fluid Mech.*, **17**, 353 (1963).
20. B. Coleman and W. Noll, *Arch. Rat. Mech. Anal.*, **3**, 366 (1960).
21. R. R. Lamonte and C. D. Han, *J. Appl. Polym. Sci.*, **16**, 3285 (1972).

Received May 25, 1972

Revised June 20, 1972